J. Nepal Chem. Soc., Vol. 23, 2008/2009

Structure of Nonionic Surfactant Diglycerol Monomyristate Micelles in Cyclohexane: a SAXS Study

Lok Kumar Shrestha*

Graduate School of Environment and Information Sciences, Yokohama National University, Tokiwadai 79-7, Hodogaya-ku, Yokohama 240-8501, Japan.
e-mail: lokkumar@hotmail.com

Abstract

Structure of nonionic surfactant diglycerol monomyristate ($C_{14}G_2$) micelles in cyclohexane has been investigated by small-angle X-ray scattering (SAXS) technique. Structural modulation of reverse micelle (RM) has been systematically studied by changing composition, temperature change and added-water. The SAXS data were evaluated by the generalized indirect Fourier transformation (GIFT) method, which gives pair-distance distribution function (PDDF). Unlike conventional poly(oxyethylene) type nonionic surfactants, $C_{14}G_2$ forms RM in cyclohexane without water addition at normal room temperature. A clear indication of one dimensional (1-D) micellar growth was found with increasing $C_{14}G_2$ concentrations. On the other hand, temperature induced cylinder-to-sphere type transition in the RM structure. The maximum dimension and the cross-sectional diameter of the RM increased upon addition of trace water indicating the formation of water pool in the reverse micellar core.

***Keywords**: Diglycerol monomyristate, small-angle X-ray scattering, reverse micelles.*

Introduction

It had reported that amphiphilic molecules undergo self-aggregation and form a variety of self-assembled structure both in polar and nonpolar solvents.[1-6] The self assembled structures and the detailed phase behavior of the conventional poly(oxyethylene)-type nonionic surfactant had extensively studied.[7-9] The self-organization of these surfactants is highly influenced by the poly(oxyethylene) chain length, surfactant concentration and the temperature. The physicochemical properties of the surfactant solutions undergo an abrupt change over a narrow concentration

*** Corresponding author***

range. The concentration at which a sharp change occurs is regarded as the critical micelle concentration (CMC). Above CMC, they form different types of micelles, vesicles or lamellar aggregates and other various liquid crystalline structures in solution. Therefore, surfactants are useful in many practical applications.

It has been found that the aggregate structures and, hence, the intrinsic geometry of an individual amphiphile has a strong influence on the shape of the micelles.[10] The different shapes of the micellar aggregates can be characterized by the critical packing parameter defined as, $cpp = v/a_o l_c$, where a_o is the effective cross-sectional area of the head group, and v and l_c are the volume and critical chain length of the hydrophobic chain, respectively. The *cpp* values for spherical, cylindrical and lamellar particle are ~1/3, 1/3< *cpp* <1/2, and 1/2< *cpp* <1, respectively.

When lipophilic surfactants are added in organic solvents, reverse micelles are formed above CMC due to dipole-dipole interaction between the hydrophilic head groups.[5] RM is generally of spherical shape with a polar head group oriented toward each other in the core and the hydrophobic groups oriented towards hydrophobic environment of nonpolar solvent. Studies on RM have attracted a significant interest over the past years because of its application in several fields. It can act as stabilizers for reactive species those are insoluble in nonpolar solvents and are also used as size controlling micro-reactor for different aqueous chemical reactions. Besides, RM is also used as template for the synthesis of nanoparticles. Previous report indicated that the structure of the nanoparticles depends on the size and shape of the template micelles.[11] Thus, controlling the structure of RM, one can control the structure of nanoparticles.

In this paper, the structure of nonionic surfactant $C_{14}G_2$ micelles in cyclohexane has been investigated using SAXS technique. SAXS measurements were performed over a wide range of compositions and temperatures. Besides, effect of added water on the RM structure has also been studied. The SAXS data were evaluated by *generalized indirect Fourier transformation* (GIFT) method to get structure of particles in real space.

Experimental Methods

The nonionic surfactant $C_{14}G_2$ was obtained from Taiyo Kagaku Co., Ltd., Yokkaichi, Japan. The surfactant was 92.9% pure and used without further purification. The main impurities are unreacted diglycerol, diglycerol di-fatty acid esters. Millipore water was used. The molecular structure of the surfactant is shown in Scheme 1.

Required amounts of 3-15 wt% of $C_{14}G_2$ solutions were prepared in CH and taken in clean and dry glass ampoules with screw cap. The samples were mixed properly by using dry thermo-bath, vortex mixer and repeated centrifugation to

achieve homogeneity. Following similar method, ternary mixtures of $C_{14}G_2$/CH/water with water composition 0.4, 0.8 and 1.2 wt% in 10 wt% $C_{14}G_2$/CH were prepared. All the samples were placed in a temperature-controlled water bath at 25 °C for few hours before SAXS measurements.

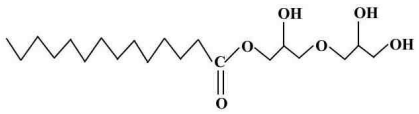

Scheme 1: Molecular structure of diglycerol monomyristate ($C_{14}G_2$).

A SAXSess camera (Anton Paar, PANalytical) is attached to a PW3830 laboratory X-ray generator with a long fine focus sealed glass X-ray tube (K_α wavelength of 0.1542 nm) was used. The apparatus was operated at 40 kV and 50 mA. An equipped Göbel mirror and a block collimator enabled us to obtain a focused monochromatic X-ray beam of Cu-K_α radiation (λ = 0.1542 nm) with a well-defined line-shape. A thermostated sample holder unit was used to control the sample temperature. The 2D scattering pattern was recorded by an imaging-plate and integrated into to one-dimensional scattered intensities $I(q)$ as a function of the magnitude of the scattering vector $q = (4\pi/\lambda)\sin(\theta/2)$ using SAXSQuant software (Anton Paar), where θ is the total scattering angle. All measured intensities were semi-automatically calibrated for transmission by normalizing a zero-q attenuated primary intensity to unity, by taking advantage of a semi-transparent beam stop. All $I(q)$ data were corrected for the background scattering from the capillary and the solvents, and the absolute scale calibration was made using water as a secondary standard. To obtain real-space structural information, SAXS data were evaluated by *generalized indirect Fourier transformation* (GIFT) method.[12-14]

In the present study, the averaged structure factor model of hard-sphere and Percus-Yevick closure relation to solve Ornstein-Zernike equation are used. The detailed theoretical description on the method is described elsewhere.[15,16]

Results and Discussion

Concentration induced 1-D micellar growth

In order to see the modulation in the structure of $C_{14}G_2$ RM, SAXS measurements were carried out on 3-15 wt% $C_{14}G_2$/CH solutions at 25 °C. Figure 1 shows the normalized scattering intensities, $I(q)$, and the corresponding pair-distance distribution function (PDDF, $p(r)$-function) deduced from the GIFT analysis of the SAXS data at different $C_{14}G_2$ concentrations at 25 °C.

Since hydrocarbon oils and hydrophobic part of the $C_{14}G_2$ surfactant are identical, SAXS selectively detects the hydrophilic core of the RM. Therefore, $p(r)$-functions must be recognized as a measure of the micellar core structure. Absence of a correlation peak in the low-q regime of the $I(q)$-q curve indicates a negligible intermicellar interaction at lower $C_{14}G_2$ concentrations. As the concentration increases, the scattering intensity increases continuously throughout the entire q-range due to the increase in the number density of the scattering particles in unit scattering volume. Minute observation of the $I(q)$-q curve reveals that the forward scattering intensity becomes suppressed with increasing $C_{14}G_2$ concentration and leads to the formation of a weak but growing interaction peak at intermediate q value (q ~ 0.9 nm^{-1}). This growing peak indicates the strong repulsive intermicellar interaction owing to the decreased osmotic compressibility of the system at higher surfactant concentration. Since the average structure factor of hard-sphere interaction potential model is generally used in the GIFT analysis, micelles cannot come to a closer distance than the diameter of a micelle. Therefore, at higher mixing fraction of surfactant, repulsive interaction comes into play as shown in the inset of Fig. 1(a).

Concentration induced one-dimensional (1-D) micellar growth can be clearly seen in the $p(r)$-function shown in Fig. 1(b). All the $p(r)$-curves exhibit typical feature of cylindrical micelles as anticipated from the pronounced peak in the low-r side and an extended tail to the higher-r side. With increasing $C_{14}G_2$ concentration from 3-15 wt%, the maximum length of the micelles (D_{max}) (as indicated by downward arrows in high-r side) increases monotonically keeping the inflection point seen after the maximum of the $p(r)$-functions in the low-r side (as indicated by a broken line), which measures the micellar cross-section semi-quantitatively practically unchanged. This confirms that the local internal structure, i.e., the cross-sectional diameter (D_c) of the micelles remains unchanged and unaffected by the change in the surfactant concentration. Thus, the results show a clear picture of 1-D micellar growth induced by composition. As we increase surfactant concentration, the *cpp* tends to decrease due to packing constraints. The decrease in the *cpp* in reverse system favors the micellar growth.

It is noteworthy to mention here that when the axial length of a cylindrical particle is at least three times longer than the cross-sectional diameter, it is possible to study the radial structure of the micelles. The core diameter for all the $C_{14}G_2$/CH systems is ~ 2.7 nm, read out from the inflection point of $p(r)$ located on the higher-r side of its sharp maximum (see Figure 1b). To confirm and quantify it more accurately, the model-free cross-section structure analysis was used and typical results are given in Fig. 2. The core cross-section diameter of ~ 2.5 nm judged from $D_{c\ max}$ in $p_c(r)$ and $R_{c\ max}$ ~ 1.3 nm in $\Delta\rho_c(r)$ for the 10 wt% $C_{14}G_2$/CH system are almost identical with those obtained in the total $p(r)$-function. Note that the cross-sectional radius ca. to 1.3 nm from the electron density profile is less than the extended length of the diglycerol molecule (hydrophilic moiety). This indicates that

the hydrophilic moiety in the micellar core is not present in its extended form (that is, it is partly soluble with the solvent CH).

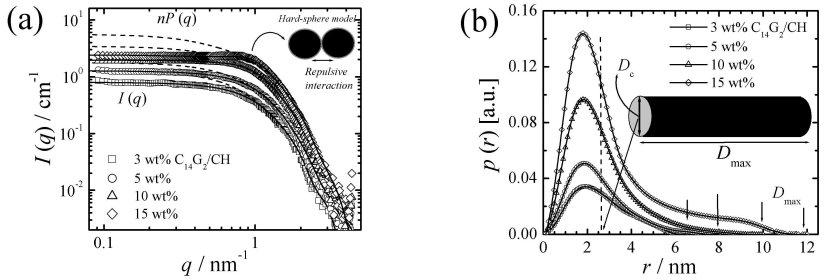

Figure 1: (a) The scattering intensities, I(q), and (b) the corresponding p(r)-function. The solid and broken lines in panel (a) represent the GIFT fit & the calculated form factor, P(q), for n particles existing in unit volume nP(q). The broken line after the maximum in the low-r side & arrows in the higher-r side of the panel (b) highlight the cross-sectional diameter & the maximum dimension of the micelle.

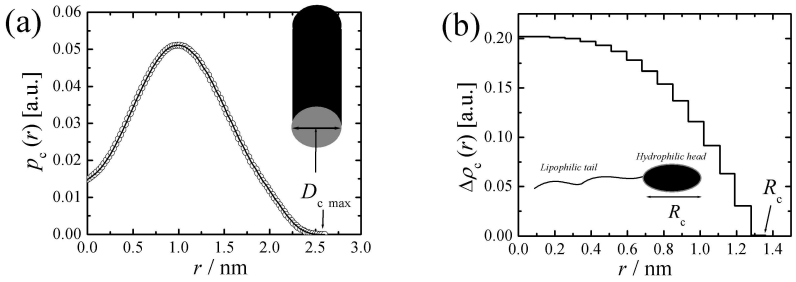

Figure 2: (a) The cross section PDDF, $p_c(r)$, for the 10 wt% $C_{14}G_2$/CH at 25 °C, and (b) the corresponding cross-section radial electron density profile $\Delta\rho_c(r)$.

Temperature induced cylinder-to-sphere transition

Figure 3 shows SAXS results for the 10 wt% $C_{14}G_2$/CH system at different temperatures. Increasing temperature decreased the scattering intensity in the forward direction {$I(q=0)$} without affecting the scattering behavior in the high-q regions. The decreasing trend of the forward intensity with increasing temperature can usually be taken as a measure of the decreasing micellar size, which may also be affected by the modified contrast as a function of temperature. The size of the RM seems to gradually decrease from ~ 10 to 4.5 nm with increasing temperature from 25 to 75°C as shown in Fig. 3(b). At 25 °C, the shape of the $p(r)$-function shows a pronounced peak in the low-r side and extended tail in the higher-r side which is a typical of long cylindrical type of particles. However, at higher temperature, the shape of the $p(r)$-function modifies into nearly symmetric bell-shaped of globular type of particles. Thus, the SAXS data unambiguously have shown that the length of

the aggregates decreases with the rise of temperature, which is essentially a cylinder-to-sphere type transition in the RM structure.

The microscopic pictures on the solution structure in the isotropic phase seem to be well connected to the miscibility of the surfactant and oils. Contrary to aqueous surfactant systems, the miscibility of oil and surfactant in nonaqueous systems increased with temperature. One of the possible reasons for the higher mutual solubility of the surfactant and oil is due to increased thermal agitation. Furthermore, with increasing temperature, the van der Walls interaction between the hydrocarbon chain of the surfactant and the oils increased. Increasing temperature enhances the penetration of oil in the surfactant chain thereby increasing *cpp* decreases the length of the RM.

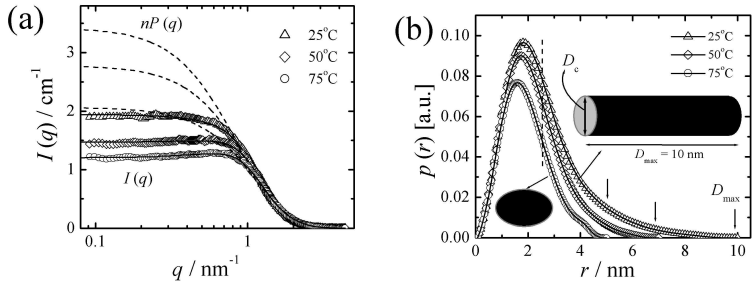

Figure 3: (a) The scattering curves I(q), of the 10 wt% $C_{14}G_2$/CH system obtained in absolute unit as a function of temperature, (b) the corresponding p(r)-functions. The schematic representation in the transition of micellar structure induced by temperature change is shown in the inset of panel (b).

Water induced 2-D micellar growth

The addition of trace polar additive like water induces micellization in nonaqueous media and thereby increases the aggregation number. The structural transition induced by the added-water in the 10 wt% $C_{14}G_2$/CH system at 25°C is well reflected in the scattering functions shown in Fig. 4(a). The forward scattering intensity is strongly enhanced and the scattering curve in the high-q region (~2 nm^{-1} as indicated by an arrow) shifts towards the forward direction upon addition of water. The corresponding real space information based on $p(r)$-function reveals that addition of water induces dramatic changes in the structure of the micelles in terms of both its maximum length (D_{max}) and the internal structure (D_c) as shown in Fig. 4(b). The addition of 0.4% water to the 10 wt% $C_{14}G_2$/CH system increases D_{max} from ~ 10 to 13 nm. Furthermore, the inflection point after the maximum shifts towards higher-r side indicating the swelling of RM. Both the D_{max} and the inflection point (broken arrows) increase with increasing water concentration. The monotonous growth of the micellar cross-section with water indicates the formation of swollen micelles with a water pool in the micellar core.[17] Thus, the added-water

causes simultaneous changes in the maximum dimension and the cross section structure of the RM.

The 2-D growth of the RM structure induced by the added-water seems to quite reasonable. As the water is added, it tends to go to the micellar core due to least miscibility of water and CH. Consequently, the water pool is formed in the micellar core, which induced cross-section growth. Besides, the water molecules may bind with hydrophilic head group by hydrogen bonding and decreases *cpp* by increasing the effective cross-sectional area of the surfactant's head group.

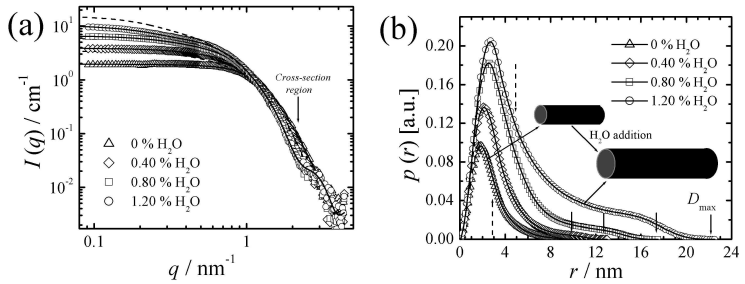

Figure 4: (a) The normalized scattering functions, I(q), as a function of water concentration obtained in absolute unit at 25°C, (b) the corresponding p(r)-function. The downward arrows in panel (b) represent the maximum length of the micelles. The upward and downward broken arrows after the maximum in the low-r side represent the cross-section diameter of water free & 1.20% water added systems, respectively.

Conclusions

The structure of nonionic surfactant micelle in organic solvent is investigated by SAXS technique, as a function of composition, temperature and added-water. The SAXS data were evaluated by GIFT method. Different shape and size of RM in $C_{14}G_2$/CH system are presented. The results obtained form the GIFT analysis of the SAXS data proved the quantitative evidence on the formation of RM in $C_{14}G_2$/CH binary system without the addition of polar additives. The spontaneous formation of RM in the studied system can be attributed to the hydrophilic nature of the diglcyerol moiety. Increasing $C_{14}G_2$ concentration favors 1-D micellar growth leading to the formation of long cylindrical type particles at higher concentrations. On the other had, temperature induced cylinder-to-sphere type transition in the RM structure. A dramatic modulation in the structure of RM is seen upon addition of traces water. Both the maximum dimension of the micelles and the cross-sectional diameter increases with water. The added-water may bind with the hydrophilic diglycerol molecules. Consequently, the effective cross-sectional area of the surfactant head group increased, and hence *cpp* decreased and favored the micellar growth. The present investigation has clearly shown the possibility to the structural control of RM and thus offers practical and fundamental implications.

Acknowledgement

LKS thanks JSPS for Postdoctoral Fellowship for Foreign Researchers.

References

1. H. Kunieda, K. Shigeta, K. Ozawa, M. Suzuki, *J. Phys. Chem. B,* 1997,**101**, 7952.
2. K. Aramaki, U. Olsson, Y. Yamaguchi, H. Kunieda, *Langmuir*,1999,**15**, 6226.
3. C. Rodriguez, H. Md. Uddin, K. Watanabe, H. Furukawa, A. Harashima, H. Kunieda, H. *J. Phys. Chem. B,* 2002, **106***,* 22.
4. L. K. Shrestha, M. Kaneko, T. Sato, D.P. Acharya, T. Iwanaga, H. Kunieda, *Langmuir,* 2006, **22***,*1449.
5. L. K. Shrestha, R.G. Shrestha, T. Iwanaga, K. Aramaki, *J. Dispers. Sci. Technol.*, 2007, **28**, 883.
6. L. K. Shrestha, T. Sato, K. Aramaki, *J. Phys. Chem B.,* 2007, **111**, 1664.
7. H. Kunieda, H. Kabir, K. Aramaki, K. Shigeta, *J. Mol. Liq.*,2001,**90**,157.
8. H. Kunieda, M. Kaneko, M. Arturo Lopez-Quintela, M. Tsukahara, *Langmuir* 2004, **20***,*2164.
9. R. Strey, R. Schomäcker, D. Roux, F. Nallet, U. Olsson, *J. Chem. Soc., Faraday Trans.*, 1990, **86**,2253.
10. J.N. Israelachvili, D. J. Mitchell, B. W. Ninham, *J. Chem. Soc. Faraday Trans.*, 1976, **72**, 1525.
11. M. P. Pileni, *Adv. Colloid Interface Sci.,* 1993, **46***,* 139.
12. G. Fritz, A. Bergmann, O. Glatter, *J. Chem. Phys.,* 2000, ***113****,* 9733.
13. O. Glatter, G. Fritz, H. Lindner. P. J. Brunner, R. Mittelbach, R. Strey, S.U. Egelhaaf, *Langmuir*, 2000, **16**, 8692.
14. B. Weyerich, J. Brunner-Popela, O. Glatter, *J.Appl.Crystallogr.* 1999,**32**,197.
15. O. Glatter, *Progr. Colloid Polym. Sci.* 1991, **84***,* 46.
16. O. Glatter, *J. Appl. Cryst.* 1980, **13***,* 577.
17. L. K. Shrestha, T. Sato, D. P. Acharya, T. Iwanaga, K. Aramaki, H. Kunieda, *J. Phys. Chem. B* 2006, **110***,* 12266.